$LiInSe_2$ nanosecond optical parametric oscillator tunable from 4.7 to 8.7 μm

Aleksey Tyazhev,[a)] Georgi Marchev,[a)] Vitaliy Vedenyapin,[b)] Dmitri Kolker,[c)]
Alexander Yelisseyev,[b)] Sergei Lobanov,[b)] Ludmila Isaenko,[b)] Jean-Jacques Zondy,[d)]
Valentin Petrov[a)]

[a]Max-Born-Institute for Nonlinear Optics and Ultrafast Spectroscopy, 2A Max-Born-Str., D-12489 Berlin, Germany;
[b]Institute of Geology and Mineralogy, SB RAS, 43 Russkaya Str., 630058 Novosibirsk, Russia;
[c]Novosibirsk State Technical University, 20 K. Marx Pr., Novosibirsk, 630072, Russia and Institute of Laser Physics (SB-RAS), 13/3 Lavren'teva Pr., Novosibirsk, 630090, Russia;
[d]Institut National de Métrologie, Conservatoire National des Arts et Métiers, 61 rue du Landy, F-93210 La Plaine St Denis, France

ABSTRACT

$LiInSe_2$ is one of the few (in the meanwhile 6) non-oxide nonlinear crystals whose band-gap (2.86 eV) and transparency enabled in the past nanosecond optical parametric oscillation in the mid-IR without two-photon absorption for a pump wavelength of 1064 nm. However, the first such demonstration was limited to the 3.34-3.82 μm spectral range with a maximum idler energy of 92 μJ at 3.457 μm for a repetition rate of 10 Hz. Now we achieved broadly tunable operation, from 4.7 to 8.7 μm, reaching maximum idler pulse energy of 282 μJ at 6.514 μm, at a repetition rate of 100 Hz (~28 mW of average power).

Key words: nonlinear crystals; lithium indium selenide; mid-infrared; optical parametric oscillator

1. INTRODUCTION

Although room temperature lasing has been reported up to ~5 μm, practical solid-state-lasers have an upper limit of ~3 μm, with the most prominent representatives being the fixed wavelength Er^{3+}-lasers and the tunable Cr^{2+}-lasers.[1] The main difficulty with such lasers consists not only in finding suitable laser transitions with long living upper state but also in the exotic pump lasers required. However, the spectral range above 3 μm in the mid-IR can be continuously covered by nonlinear frequency down-conversion using powerful laser sources in the near-IR. Oxide-based crystals, for example phosphates and arsenates belonging to the $KTiOPO_4$ (KTP) family of isomorphs, or iodates, niobates and tantalates like $LiIO_3$, $LiNbO_3$, $KNbO_3$, $LiTaO_3$, as well as all their periodically poled counterparts, can be pumped by widely-spread high-power diode-pumped laser systems, such as Nd:YAG, and perform well up to 4 μm, but their performance at longer wavelengths is dramatically affected by the onset of multi-phonon mid-IR absorption. Since nonlinear frequency conversion is intensity dependent process, high efficiency can be expected only using pulsed laser sources (femtosecond to nanosecond). At practical pump intensities, most of the chalcogenide mid-IR nonlinear crystals will suffer then two-photon absorption (TPA) at the pump wavelength of 1064 nm because of their low band-gap. Although TPA is the major limitation, in many cases residual absorption at the pump wavelength or insufficient birefringence for phase-matching pose additional constraints. Thus, from the I-III-VI_2 chalcopyrite crystals, only $AgGaS_2$ but not $AgGaSe_2$, can be phase-matched and pumped without TPA at 1064 nm, however, sulfides exhibit in general substantially lower second order nonlinearity than selenides. II-IV-V_2 chalcopyrites offer superior properties in comparison to the I-III-VI_2 chalcopyrite crystals in terms of nonlinearity, low scattering losses, hardness, and thermo-optical and thermo-mechanical parameters,

Nonlinear Frequency Generation and Conversion: Materials, Devices, and Applications IX,
edited by Peter E. Powers, Proc. of SPIE Vol. 7582, 75820E · © 2010 SPIE
CCC code: 0277-786X/10/$18 · doi: 10.1117/12.839893

but even the most developed compound, $ZnGeP_2$, requires pump wavelengths near 2 µm (less common sources like Tm- or Ho-lasers) in order to avoid two-photon and residual absorption as well as to enable phase-matching. The TPA problem precludes also the pumping of the newly developed orientation-patterned GaAs at wavelengths near 1 µm. In fact, there are only few candidates for such down-conversion devices pumped near 1064 nm, the properties of which were compared in Ref. 2 taking into account the TPA, residual absorption, birefringence, effective nonlinearity, thermal conductivity, and limitations related to the growth, availability and some opto-mechanical properties.

Although femtosecond and picosecond pulses are associated with much higher peak intensities, it is difficult to achieve simultaneously high output energies and conversion efficiency because of limitations related to the spectral acceptance or higher order dispersion and nonlinear effects. Thus nanosecond optical parametric oscillators (OPOs) seem to possess the best potential for achieving high average power and single pulse energy. Such OPOs, pumped in the 1 µm range, have been demonstrated, however, only with 6 of the 14 compounds analyzed in Ref. 2: Ag_3AsS_3,[3-5] $AgGaS_2$,[6-9] $HgGa_2S_4$,[10-12] the solid solution $Cd_xHg_{1-x}Ga_2S_4$,[13-14] $LiInSe_2$,[15] and very recently $CdSiP_2$.[16] The relevant properties of these crystals are summarized in Table 1, where a specific pump (1064 nm) and idler (6.45 µm) wavelengths are selected for comparison.

Table 1. Compilation of important properties of nonlinear crystals for which OPO operation with ~1 µm pump has been demonstrated. The citations in column 2 refer to the Sellmeier equations used. The effective nonlinear coefficients d_{eff} (column 3) are calculated at the corresponding phase-matching angle θ or φ (column 2), the nonlinear tensor components, d_{il}, used for this calculation were derived from the literature (column 6) applying Miller's rule (column 7). The wavelength λ_F (fundamental) at which the nonlinear coefficients have been estimated by SHG is also included in column 6. Citations in the first column refer to the whole row.

Crystal Point group [Reference] Plane	θ / φ [°] (Interaction)	d_{eff} [pm/V]	Thermal conductivity [W/mK]	Band-gap E_g [eV]	Miller's δ [pm/V] or d_{il} [pm/V] @ λ_F for SHG	+ Miller's correction [pm/V]
$AgGaS_2$ $\bar{4}2m$	40.50 (oo-e) 45.53 (eo-e) [17]	8.86 13.65	1.4 //***c*** 1.5 ⊥***c*** [18]	2.70 [19]	δ_{36}=0.12 [20]	d_{36}=13.65
$HgGa_2S_4$ $\bar{4}$	45.87 (oo-e) 51.21 (eo-e) [10]	15.57 21.18	2.49-2.85 //***c*** 2.36-2.31 ⊥***c*** [21]	2.79 [21]	d_{36}=27.2 @ 1064 nm [21]	d_{36}=24.56
$Cd_xHg_{1-x}Ga_2S_4$ (θ=90°, x=0.55) $\bar{4}$	90.00 (oo-e) [21]	24.94	1.8-1.92 //***c*** 1.62-1.81 ⊥***c*** (x=0.27-0.3) [21]	3.22 (x=0.55) [21]	d_{36}=27.2 @ 1064 nm [21]	d_{36}=24.94
$LiInSe_2$ xz $mm2$ xy [22]	36.97 (oo-e) 41.62 (eo-e)	7.26 10.57	4.7-4.5 //***x*** 4.7-4.8 //***y*** 5.5-5.8 //***z***	2.86	d_{31}=11.78 d_{24}=8.17 @ 2300 nm	d_{31}=12.08 d_{24}=8.65
$CdSiP_2$ $\bar{4}2m$	80.46 (oo-e) [23]	90.99	13.6 [2]	2.2-2.45 [24]	d_{36}=84.5 @ 4.56 µm [2]	d_{36}=92.27
Ag_3AsS_3 $3m$ [25]	22.04 (oo-e) 24.01 (eo-e) 65.63 (oe-e)	22.89 16.44 3.35	0.113 //***c***, 0.092 ⊥***c***	2.2	d_{31}=10.4 d_{22}=16.6 @ 10.6 µm	d_{31}=12.34 d_{22}=19.70

$AgGaS_2$ (AGS) is the only commercially available crystal from Table 1. Besides its modest nonlinearity, it exhibits low thermal conductivity and strongly anisotropic thermal expansion. $HgGa_2S_4$ shows improved nonlinearity but the growth of this crystal in large sizes with sufficient homogeneity is still problematic and several phases exist. $Cd_xHg_{1-x}Ga_2S_4$, with x=0.55 adjusted to have non-critical phase-matching for the selected process, is a solid solution in the system $HgGa_2S_4 - CdGa_2S_4$ and can be grown in larger sizes but its composition cannot be maintained constant. Li-compounds exhibit the largest band-gaps of all mid-IR crystals but their nonlinear coefficients are relatively low. Unlike the AGS chalcopyrite, they crystallize in the β-$NaFeO_2$ wurtzite-type structure (orthorhombic *mm*2 symmetry). The interest in $LiInSe_2$ (LISe), the Li compound with highest nonlinearity, is motivated by its superior thermo-mechanical properties:[22] quasi-isotropic expansion, thermal conductivity ~5 W/mK (~3 times higher than in AGS), and smaller thermo-optic coefficients as well as higher damage threshold than AGS, which are important for average power scaling. Ag_3AsS_3

(proustite) is an archive crystal, included in Table 1 only for completeness. Being one of the first mid-IR crystals studied, its development has been cancelled in favor of the chalcopyrites such as AGS, because of the poor thermo-mechanical properties and low laser damage threshold. $CdSiP_2$ is a II-IV-V_2 chalcopyrite with negative birefringence whose growth technology was developed only very recently. It possesses unique properties for down conversion to the mid-IR at pump wavelengths near 1 µm and outperforms all other crystals in all aspects, not only those used for comparison in Table 1, but also in terms of hardness, damage threshold or anisotropy of the thermal expansion, as well as the possibility of non-critical phase-matching with maximized effective nonlinearity without being a solid solution. However, a practical upper limit of 6.5 µm for the idler wavelength can be assumed due to the onset of intrinsic multi-phonon absorption: This defines a potentially interesting spectral range for $CdSiP_2$ of only 4 to 6.5 µm.

Table 2. Development of 1-µm pumped OPOs based on non-oxide materials. L: crystal length, SF: single-frequency, T_P: pump pulse duration (FWHM), SP: single pump pass, DP: double pump pass, N-C: non-collinear, Q-D: quasi-degeneracy, SR: singly resonant, DR: doubly resonant, TT: temperature tuning, NC: non-critical, NM: not measurable, λ_I: idler wavelength (tunability), E_I: maximum idler energy, I_P: maximum applied or damage level pump intensity. $Cd_xHg_{1-x}Ga_2S_4$ and $CdSiP_2$ operated under NC conditions with tuning by variable composition (x=0.21-0.25 in Ref. 14) in the case of $Cd_xHg_{1-x}Ga_2S_4$ and at fixed wavelength for $CdSiP_2$.

Crystal, Type	L [mm]	λ_P [nm], Mode	Rep. rate [Hz]	T_P [ns]	SP/ DP	λ_I [µm]	E_I [µJ] @ λ_I	Peak I_P [MW/cm^2], Limits, commments	Year	[Ref.]
Ag_3AsS_3 I (e-oo)	3.8	1064 TEM_{00}	2000	200	SP	~2.128, Q-D, DR	NM	0.45, surface and/or coating damage	1970	[3]
Ag_3AsS_3 I (e-oo)	10	1065 TEM_{00}, SF	2	26	SP	2.13-2.56 Q-D, DR	12.5 @ 2.13 µm	8.5, safe 19, surface damage	1972	[4]
Ag_3AsS_3 I (e-oo)	10	1065 TEM_{00}	2	25	SP, N-C	2.13-8.5, SR	2.5 @ 4.5 µm	see above	1973	[5}
$AgGaS_2$ I (e-oo)	20	1064 TEM_{00}	10	20	SP	2.128-4, SR	250 @ 2.128 µm	10, surface damage	1984	[6]
$AgGaS_2$ I (e-oo)	20	1064	10	10.9	DP	2.77-4.2, SR	120 @ 3.5 µm	<30, surface damage after 50 shots	1997	[7]
$AgGaS_2$ II (e-oe)	20	1064, TEM_{00}	10	20-30	DP	3.9-11.3, SR	372 @ 6 µm	10, surface damage	1999	[8]
$AgGaS_2$ I (e-oo)	20	1064, TEM_{00}	1	15	DP	2.6-5.3, SR	620 @ 4 µm	34, mirror damage	2006	[9]*
$HgGa_2S_4$ II (e-oe)	8	1064	10			~3.7-4.5, SR		40, surface damage	1998	[10]
$HgGa_2S_4$ I (e-oo)	6	1064, TEM_{00}	10	30	SP	2.3-4.4, SR	360 @ 2.37 µm	40, surface damage, single shot (extracavity)[26]	2003	[11]
$HgGa_2S_4$ I (e-oo)	6	1064, TEM_{00}	10	15	DP	3.75-4.65, SR, +TT	~65@ 4.35 µm		2009	[12]
$Cd_xHg_{1-x}Ga_2S_4$ I (e-oo)	10.9-11.6 x=0.22-0.56	1064, TEM_{00}	10	30	SP	3.16-8.9, SR, NC for x=0.56	270 @ 5.76 µm 110 @ 8.9 µm	damage threshold: 6 fold that of AGS x=0.35 (extracavity) T_P=9 ns, single shot	2004	[13]
$Cd_xHg_{1-x}Ga_2S_4$ I (e-oo)	11 x=0.21-0.25	1064, TEM_{00}	10	22	SP	2.85-3.27, SR, NC	400 @ 3.03 µm		2005	[14]
$LiInSe_2$ II (e-oe)	17	1064	10	10	DP	3.34-3.82, SR	92 @ 3.457 µm	40, safe (extracavity) 54, coating damage[27]	2005	[15]
$LiInSe_2$ II (e-oe)	17.6, 24.5	1064	100	14	DP	4.65-7.5, 5.45-8.7, SR	282 @ 6.5 µm	>21, surface damage limit (intracavity) 45, coating damage (extracavity)	2009	This work
$CdSiP_2$ I (e-oo)	8	1064	10	14	DP	6.2, SR, NC	470 @ 6.2 µm	25, AR coating damage (intracavity)	2009	[16]

*related data can be found in Ref. 28,29 but the results in terms of output energy and tuning range do not represent an improvement in comparison with Ref. 9.

Table 2 summarizes the OPO results demonstrated so far with the 6 crystals from Table 1. Q-switched Nd:YAG lasers (Nd:$CaWO_4$ in Ref. 4,5) have been used for pumping. Simple two-mirror cavities were employed in all cases.

In this work we report broadband operation of a 1064 nm pumped LISe OPO, tunable from 4.65 to 8.7 μm using a single crystal sample. Pumping at a repetition rate of 100 Hz and the absence of thermal effects enabled us to increase the average power by more than an order of magnitude at wavelengths much longer than in the initial demonstration.[15]

2. EXPERIMENTAL SETUP AND CRYSTAL SAMPLES

The OPO cavity used is shown in Figs. 1 and 2. It consisted of two plane mirrors with a separation between 18.5 and 27.5 mm, depending on the LISe crystal used. The rear total reflector, TR, was an Ag-mirror (Balzers) with a reflection of >98.5% at the pump, signal and idler wavelengths. In the tuning range studied in the present work, the output coupler, OC, had a transmission of 18-22% at the signal and ~73-84% at the idler wavelength, hence, the OPO can be considered as singly resonant with double pass pumping. However, the signal was not totally reflected by the output coupler to avoid extreme intracavity fluence that could damage the crystals. The LISe crystals were pumped through the output mirror which had a transmission of 82% at 1064 nm. The beams were separated by the pump bending mirror, BM, which had high reflection for the pump (R=98% for p-polarization) and transmitted ~67% (p-polarization) at the idler wavelengths, respectively. Both the plane-parallel output coupler, OC, and the bending mirror, BM, were on ZnSe substrates with uncoated rear surfaces.

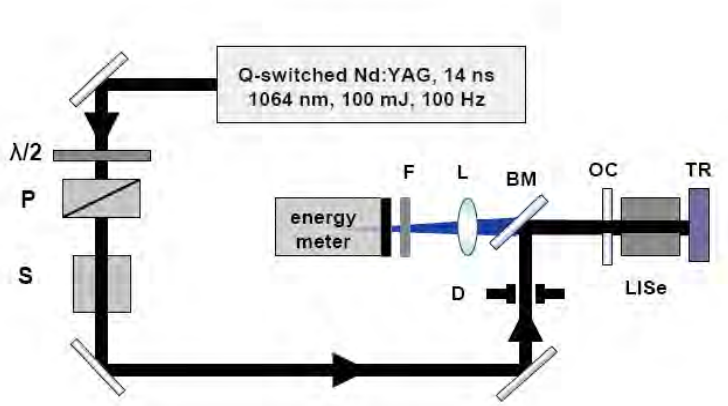

Fig. 1 Experimental setup of the LISe OPO. $\lambda/2$: half-wave plate, P: polarizer, S: mechanical shutter, F: 2.5 μm cut-on filter, L: 10 cm MgF_2 lens, D: diaphragm, BM: bending mirror, OC: output coupler, TR: total reflector.

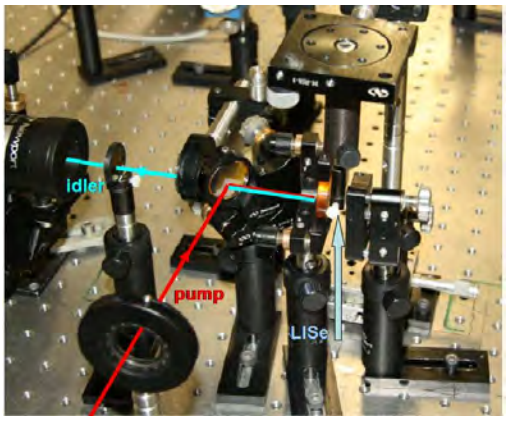

Fig. 2 Photograph of the compact OPO setup.

The pump source was a diode-pumped, electro-optically Q-switched Nd:YAG laser (Innolas GmbH, Germany) optimized for a repetition rate of 100 Hz. According to the specifications, its linewidth amounts to 1 cm^{-1}, M^2 is <1.5 and the divergence is <0.5 mrad. The laser generated 100 mJ, 14 ns (FWHM) pulses with an average power of 10 W. The measured energy stability was +/-1%.

A mechanical shutter (S) with an aperture of 8 mm, operating up to 50 Hz (nmLaser), was employed to reduce the repetition rate and thus the average pump power. A combination of a half-wave plate, $\lambda/2$, and a polarizer, P, served to adjust the pump energy. The pump laser was protected by a Faraday isolator and the separation to the OPO was large enough to avoid feedback during the Q-switching process. The pump beam was not focused and had a Gaussian waist of w~1.9 mm in the position of the OPO. The output of the OPO, behind the bending mirror, BM, was detected by a calibrated pyroelectric energy meter positioned in front of the focus of a 10-cm MgF_2 lens, L. Only the idler energy was measured, the residual pump radiation and the signal were blocked by a 2.5 μm cut-on filter, F.

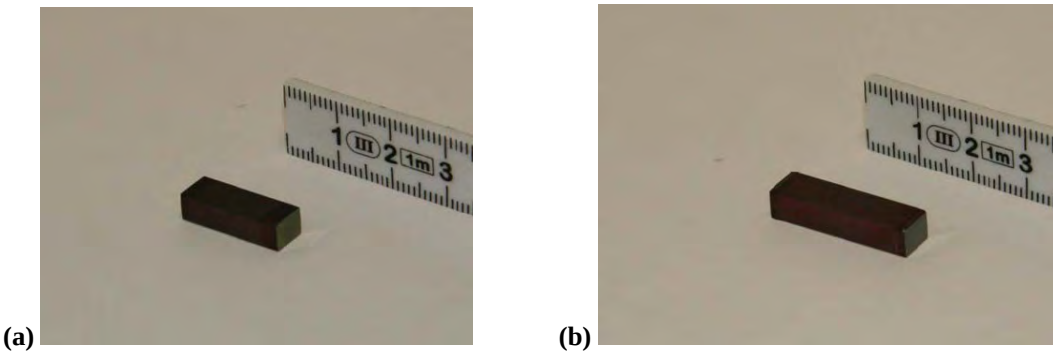

Fig. 3 AR coated samples of $LiInSe_2$ used in the present work: sample A (a) and sample B (b).

The samples used in the present study, see Fig. 3, were grown from an oriented seed by the vertical two-zone furnace Bridgman technique. They were cut for propagation in the *x-y* plane, type-II e-oe phase-matching, which is characterized by maximum effective nonlinearity, d_{eff}.[22] One sample (A) was cut at φ=41.6° for idler wavelength ~6.5 μm at normal incidence. It had an aperture of 5 mm (along *z*-axis) × 6.5 mm and a length of 17.6 mm. This sample was AR-coated with a single layer of YF_3 for high transmission at 1064 nm and in the 1.15-1.35 μm signal range, Fig. 4. We measured average surface reflectivity of 2.8% at 1064 nm and 1.8% at 1600 nm. From the measured transmission of 71% at 1064 nm and 85% at 1600 nm, we estimated effective absorption (including scatter) of 16%/cm at 1064 nm and 7%/cm at 1600 nm.

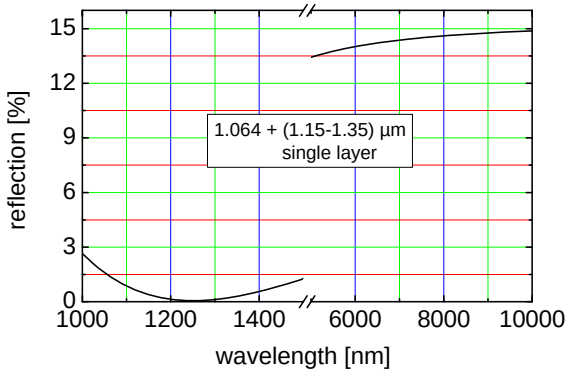

Fig. 4 Single-layer AR-coating design used for the $LiInSe_2$ samples.

The second sample (B) was cut at φ=34° for idler wavelength ~8.8 μm at normal incidence. It had an aperture of 5 mm (along *z*-axis) × 7 mm and a length of 24.5 mm. This sample was AR-coated with the same single layer for high transmission at 1064 nm and in the 1.15-1.35 μm signal range. However, due to some failure in the coating process, the difference in the residual reflectivity of the two surfaces was more pronounced. One surface had substantially higher (5% at 1064 nm and 4.5% at 1600 nm) reflection than the other (1% at 1064 nm and <1% at 1600 nm). From the measured transmission of 67.7% at 1064 nm and 82% at 1600 nm, we estimated for sample B, effective absorption (including scatter) of 14%/cm at 1064 nm and 6%/cm at 1600 nm, which are very similar to the estimates for sample A.

3. RESULTS AND DISCUSSION

We studied the input/output characteristics of the OPO, including the oscillation threshold, at normal incidence and minimum possible cavity length. The tuning curve required tilting of the crystal and the corresponding cavity length was slightly increased.

The thresholds measured for cavity length of 18.5 mm (sample A) and 25.5 mm (sample B) amounted to 6.8 mJ and 7.9 mJ, energy incident on the crystals, respectively. These values correspond to average fluence of 0.06 J/cm^2 and 0.07 J/cm^2 or pump intensity of 4.3 MW/cm^2 and 5 MW/cm^2. The peak on-axis values for the fluence and the intensity are two times higher. The threshold can be calculated by using Brosnan & Byer's formula[30] for a singly resonant OPO with recycled pump. We used the exact experimental parameters, correcting for the pump beam absorption after the first pass and assuming equal (averaged for signal and idler) absorption of 5%/cm^{-1} for the resonated wave. From the nonlinear coefficients of LISe, rescaled using Miller's rule,[2] we calculated an effective nonlinearity of d_{eff}=10.6 pm/V (φ=41.6°, sample A) and 11 pm/V (φ=34°, sample B), see Table 1. The results for the threshold pump fluence were 0.23 J/cm^2 and 0.15 J/cm^2 for sample A and B, respectively. These values correlate better with the experimental peak (on-axial) values which can be explained by the fact that oscillation starts in the central part of the pump beam. Deviations and the fact that sample B had in fact a higher oscillation threshold than sample A may have several reasons: the losses at the exact signal and idler wavelengths were unknown and we interpolated them to 6%cm^{-1} at the signal and assumed 4%cm^{-1} at the idler wavelength in accordance with Ref. 15, eventually these losses, in particular for sample B, could be higher; besides for the pump, the residual reflections at the crystal faces were neglected; and finally the partial resonance of the idler is not taken into account by the theory. Having in mind all such assumptions, the correspondence between theory and experiment can be considered as satisfactory.

At a pump level of about two times the pump threshold we investigated the dependence of the output power on the repetition rate in the range 10-100 Hz. Fluctuations were within the experimental error and we conclude that there is no such dependence. This result was rather unexpected since the present samples had in fact larger residual absorption than the one used in the initial work[15] at shorter idler wavelengths. This fact can be explained by the weaker thermal lensing in the case of larger beam sizes. The measurements were performed at 100 Hz with the shutter removed (Fig. 1).

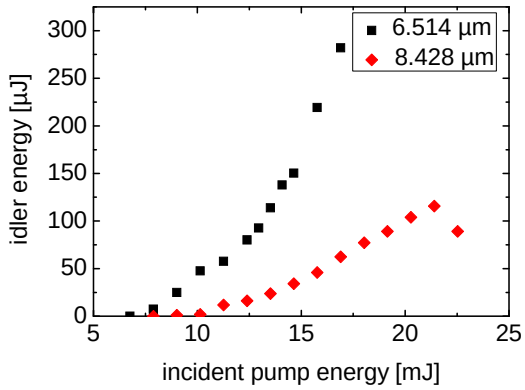

Fig. 5. Output idler energy with LISe sample A (black squares) and sample B (red diamonds) versus pump energy at 1064 nm, incident on the crystals. The curves are recorded at normal incidence with cavity lengths of 18.5 and 25.5 mm, respectively. The last point in case B denotes a surface damage.

The input/output characteristics for the two samples are shown in Fig. 5. Maximum energies of 282 µJ at 6.514 µm and 116 µJ at 8.428 µm were measured. These values correspond to external quantum conversion efficiencies of 10.3% and 4.3%, respectively. The above wavelengths deviate from the calculated ones being longer for sample A and shorter for sample B. However, the deviations at the signal wavelengths, from the measurement of which the idler wavelengths were calculated, were only about 3 nm and 5 nm, respectively. The maximum average power at 100 Hz amounts to 28 mW. This is an improvement of more than an order of magnitude in comparison to our initial work, where ~2.5 mW at 3457 nm were achieved at lower repetition rates.[15] Since OPO operation with any chalcogenide crystal is confined to a narrow pump power range between the oscillation threshold and the damage threshold this fact emphasizes the importance of the good spatial profile and the pulse-to-pulse stability of the diode-pumped pump source.

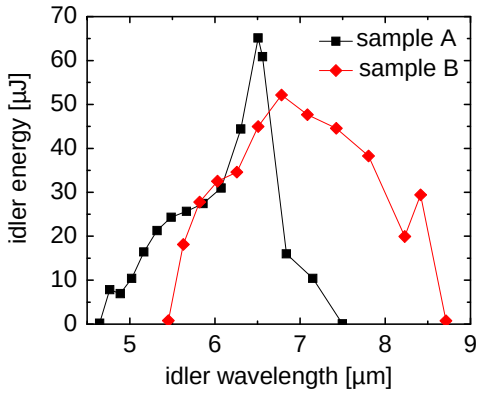

Fig. 6 Tuning OPO curves recorded for the two LISe samples at fixed pump energy.

The OPO linewidth was measured at the signal wavelength of 1272 nm using a 1-mm-thick Ag-coated CaF_2 Fabry-Perot etalon. It was ~58 GHz (~1.9 cm^{-1}). This is 2 times less than the spectral acceptance for the three-wave nonlinear process assuming narrow-band pump. The pulse-to-pulse stability for the idler pulses measured at maximum output level was +/- 5%. The pulse duration at the same signal wavelength, measured with a fast (0.7 ns) InGaAs photodiode, was 7 ns.

The tuning curves (Fig. 6) were recorded by lengthening the cavity to 20.5 mm (sample A) and 27.5 mm (sample B) and tilting the crystals in the critical plane (rotation about the z-axis). The pump energy was 11.8 mJ for sample A and 16.9 mJ for sample B. Note that the upper limit of the tunability is determined by the LISe absorption which, for such sample lengths, sets on from about 8 µm, and is not related to the optics used (the thin MgF_2 lens was substituted by a BaF_2 lens to check this). The point which deviates from the smooth dependence for sample B is near 8.428 µm, corresponding to normal incidence, which can be explained by some enhancement of the feedback by the partial reflection of the crystal faces. Thus we showed that the full transparency range of LISe can be utilized using an OPO pumped at 1064 nm, however, in order to extend the tunability up to 12 µm and more, shorter crystal samples will be needed in addition to reduction of the residual crystal loss. This in turn means that the OPO should be operated at higher pump levels which will require solution of the surface damage problem.

4. OPTICAL DAMAGE

Surface damage of LISe was observed with both OPO active elements and studied also with four 1 mm thick plates, cut in the same direction as sample B. Two of these plates were only polished and the other two had AR-coating on one of their faces only. The results of the extracavity damage tests at 1064 nm using the same pump source without focusing can be summarized as follows.

For uncoated and AR-coated LISe plates, complete damage (surface and crack) occurs for 14 ns long pulses at 1064 nm and 100 Hz within seconds/minutes for 44-52 mJ incident energy, on-axis fluence of 0.78-0.92 J/cm^2 (56-66 MW/cm^2 peak on-axis pump intensity).

In several cases irreversible whitened spots (surface deterioration) were observed starting from 29 mJ, corresponding to an on-axis fluence of 0.5 J/cm^2 or a peak on-axis intensity of 36 MW/cm^2. This is the minimum fluence value for which such kind of damage was observed, and there is obvious dependence on the position and the sample. For increasing pump levels, the whiter spots changed slightly in diameter and preserved their colour, until complete damage occurred. The whiter spots appear on uncoated surfaces, however, they occur also on AR-coated surfaces, presumably beneath the layer. In most of the cases they occurred at higher pump energies and in one of the uncoated test plates they did not occur at all, until complete damage was observed at 52 mJ (Fig. 7b), which seems to indicate that this effect is related to the polishing/coating procedure since all samples were from the same LISe boule.

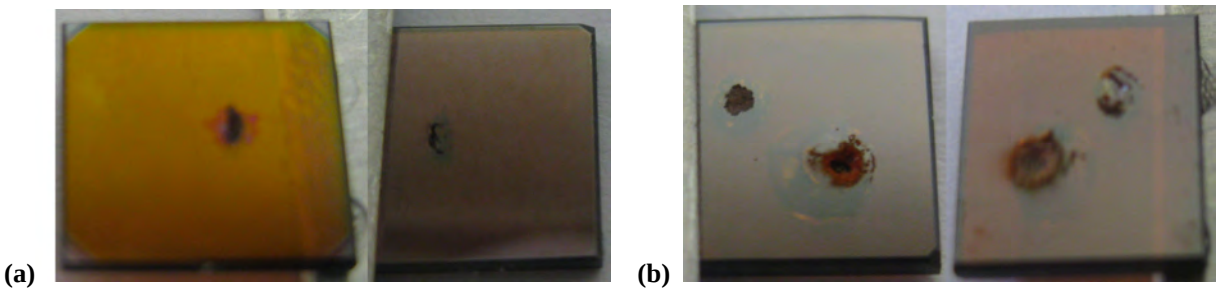

Fig. 7 Damage of the AR-coated front surface (left) and the uncoated rear surface (right) of a LISe test plate after illumination with 3000 pulses of 50 mJ energy (a) and damage of both sides of an uncoated LISe test plate at 52 mJ single pulse energy after 3000 (small spots) and 10000 (large spots) pulses (b).

No reliable information could be obtained on gray track formation which seems not to be the limiting factor in the temporal regime studied. However, many point defects could be seen with a microscope in all samples, inside the bulk and on the surface, Fig. 8. Their concentration differs and possibly correlates with the different damage thresholds observed.

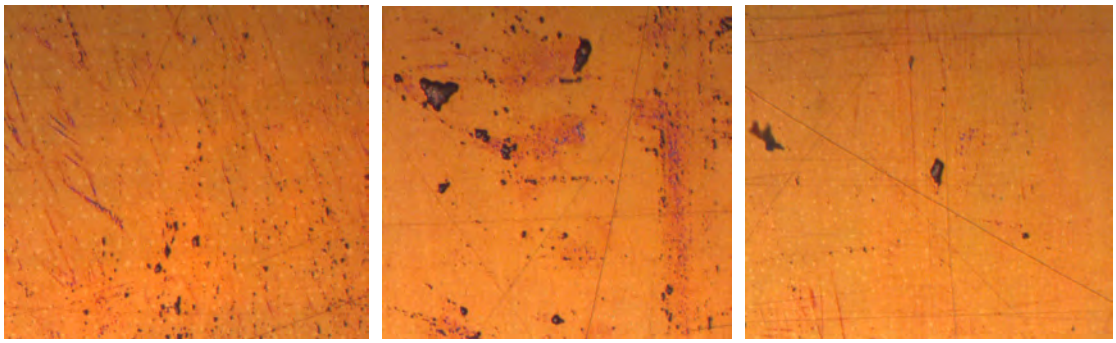

Fig. 8 Microscope pictures of surface segments of one of the uncoated test plates of LISe before the damage tests (size of the above pictures is appr. 2 mm × 2 mm).

In principle the AR-coating applied seems to be sufficiently resistant for OPO operation and in some cases the surface damage threshold was higher for the AR-coated surface. But the quality of the coating is not reproducible as evidenced in the OPO experiment, in which always one of the surfaces (the one with higher residual reflection) got damaged at lower pump levels, independent whether it was a front or rear surface with respect to the pump.

The lowest pump level at which surface damage to OPO sample A in the form of whitened spots on the coating (or beneath it), were observed, was a peak on-axial pump intensity of 16 MW/cm^2. This corresponds to operation roughly two times above the threshold and strong signal field is already present in the cavity. By translating the sample in transversal direction, we observed several times the same kind of damage to the same surface, the one with higher residual reflectivity of the AR-coating, independent of the orientation of the sample with respect to the pump beam (entrance or exit surface). No damage occurred to the other surface of the sample.

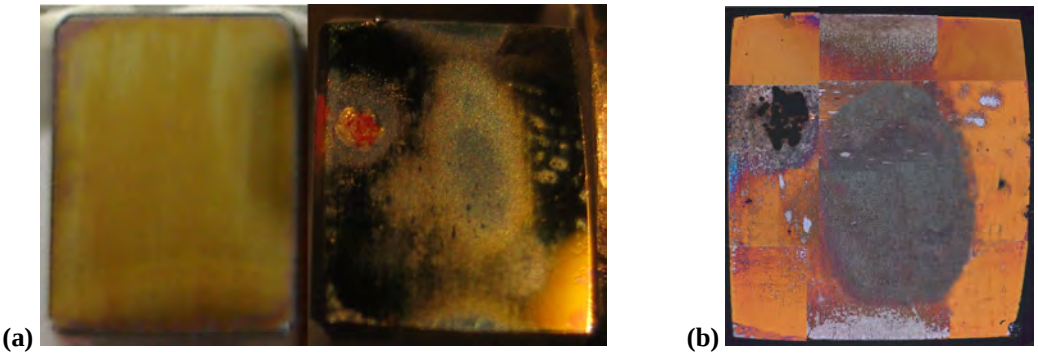

Fig. 9 Lower-reflecting (left) and higher-reflecting (right) surface of the damaged LISe OPO element (a) and 12 microscope images of the severely damaged higher-reflecting surface combined into a single picture.

The same sample A was studied for damage also extracavity, using the same pump source and fresh positions. The tests were performed for 60 s (6000 shots). Again the same surface had low damage threshold although it was always an exit surface. The damage threshold for the occurrence of similar whitened spots was 23 MW/cm^2. Full damage to this surface (coating destroyed and crater appeared, see Fig. 9a) occurred at 45 MW/cm^2. At this same intensity level, the first whitened spot on the other surface (the one with lower residual reflectivity) was observed. Hence, this value is included in Table 2 as a realistically achievable damage resistivity level of this type of coating.

It can be only speculated why damage of the two OPO samples in the form of whiter surface spot occurred at much lower pump energy (10-15 mJ) when inside the cavity. Nevertheless, the presence of such spots did not affect the OPO performance until the damage developed further as can be seen from Fig. 5. Complete damage was also observed at lower levels (15-20 mJ) inside the cavity but could be a consequence of already existing whiter spot. There are two possibilities: either contribution from the resonated signal wave (as reported for other crystals[8]) or simply low quality of this AR-coating. Experiments outside the cavity indicated lower damage of the surface with higher residual reflection, also lower threshold for whitening, so it seems more probable that this surface was simply of lower quality and that is why it got damaged although it was not always the front surface in the OPO. The different damage resistivity of the two surfaces could be attributed to the fact that after AR-coating one of the surfaces, the other one was not repolished. In the future we plan to polish the two crystal faces independently prior to their coating. Comparing the results with coated and uncoated surfaces one can expect that, for the present quality of the grown material, optimization of the AR-coating process could allow the safe use of peak on-axis intensities of about 50 MW/cm^2 or incident pump energy of roughly 40 mJ. Once the problem with the reproducibility of the AR-coating is solved one can expect substantial improvement of the OPO performance.

For other types of OPOs pumped by mode-locked lasers near 1 μm (synchronously pumped OPOs or SPOPOs) which operate at ~100 MHz repetition rates, it is essential to know the continuous-wave (CW) optical damage threshold of LISe. To this aim we tested one of the uncoated 1-mm thick plates with a CW Nd:YVO_4 laser operating at 1064 nm. With a 30-mm best shape lens we measured a waist diameter in the focus of $2w_0$=18 μm and estimated M^2=1.6. The maximum power applied, measured after the lens, was 8.5 W which gives an average intensity of 3.3 MW/cm^2 in the focus. By translating the plate through the focus and averaging two tests we estimated then a damage threshold of ~6 MW/cm^2 in terms of peak on-axis intensity. The bulk damage was in the form of dark spots inside the sample.

5. CONCLUSION

In summary, we demonstrated nanosecond OPO operation with LISe crystal in the mid-IR wavelength range above 4 µm extending up to 8.7 µm for the idler wave. The maximum idler pulse energy of 282 µJ at ~6.5 µm corresponds to an average power of ~28 mW at a repetition rate of 100 Hz. This compares well with the 372 µJ at 6 µm reported with an AGS OPO.[8] Further scaling is possible provided better polishing and AR-coating processes are developed. One of main challenges remains, however, the reduction of the residual losses in the clear transparency range of LISe because only after solving this problem the better thermo-mechanical characteristics of this material will allow to outperform the more conventional chalcopyrite AGS.

ACKNOWLEDGMENTS

The research leading to these results has received funding from the European Community's Seventh Framework Programme FP7/2007-2011 under grant agreement n° 224042. We acknowledge also support from DLR (International Bureau of BMBF) under project RUS 08/013 and from DAAD, Michail-Lomonosov-Programme (D. K.).

REFERENCES

[1] Kaminskii, A. A., "Laser crystals and ceramics: recent advances," Laser & Photon. Rev. **1**, 93-177 (2007).

[2] Petrov, V., Noack, F., Tunchev, I., Schunemann, P., and Zawilski, K., "The nonlinear coefficient d_{36} of $CdSiP_2$," Proc. SPIE **7197**, 7197-21/1-8 (2009).

[3] Amman, E. O. and Yarborough, J. M., "Optical parametric oscillation in proustite," Appl. Phys. Lett. **17**, 233-235 (1970).

[4] Hanna, D. C., Luther-Davies, B., Rutt, H. N., and Smith, R. C., "Reliable operation of a proustite parametric oscillator," Appl. Phys. Lett. **20**, 34-36 (1972).

[5] Hanna, D. C., Luther-Davies, B., and Smith, R. C., "Singly resonant proustite parametric oscillator tuned from 1.22 to 8.5 µm," Appl. Phys. Lett. **22**, 440-442 (1973).

[6] Fan, Y. X., Eckardt, R. C., and Byer, R. L., "$AgGaS_2$ infrared parametric oscillator," Appl. Phys. Lett. **45**, 313-315 (1984).

[7] Phua, P. B., Wu, R. F., Chong, T. C., and Xu, B. X., "Nanosecond $AgGaS_2$ optical parametric oscillator with more than 4 micron output," Jpn. J. Appl. Phys. **36**, L1661-L1664 (1997).

[8] Vodopyanov, K. L., Maffetone, J. P., Zwieback, I., and Rudermann, W., "$AgGaS_2$ optical parametric oscillator continuously tunable from 3.9 to 11.3 µm," Appl. Phys. Lett. **75**, 1204-1206 (1999).

[9] Wang, T.-J., Kang, Z.-H., Zhang, H.-Z., He, Q.-Y., Qu, Y., Feng, Z.-S., Jiang, Y., Gao, J.-Y., Andreev, Y. M., and Lanskii, G. V., "Wide-tunable, high energy $AgGaS_2$ optical parametric oscillator," Opt. Express **14**, 13001-13006 (2006).

[10] Takaoka, E. and Kato, K., "Tunable IR generation in $HgGa_2S_4$," Conference on Lasers and Electro-Optics CLEO'98, San Francisco (CA), USA, May 3-8, 1998, paper CWF39, 1998 OSA Technical Digest Series Vol. 6, pp. 253-254.

[11] Badikov, V. V., Don, A. K., Mitin, K. V., Seregin, A. M., Sinaiskii, V. V., and Schebetova, N. I., "A $HgGa_2S_4$ optical parametric oscillator," Quantum Electron. **33**, 831-832 (2003) [transl. from Kvantovaya Elektron. **33**, 831-832 (2003)].

[12] Mangin, J, Mennerat, G., Gadret, G., Badikov, V., and de Miscault, J.-C., „Comprehensive formulation of temperature-dependent dispersion of optical materials: illustration with case of temperature tuning of a mod-IR $HgGa_2S_4$ OPO," J. Opt. Soc. Am. B **26**, 1702-1709 (2009).

[13] Badikov, V., Fintisova, A., Panutin, V., Sheina, S., Scherbakov, S., Shevyrdyaeva, G., Don, A., Mitin, K., Schebetova, N., Seryogin, A., Sinaisky, V., Kuzmin, N., Laptev, V., Malinovsky, A., Ryabov, E., Mangin, J., Gadret,

G., Jules, J.-C., Mennerat, G., Pasquer, C., and de Miscault, J.-C., "$Hg_{1-x}Cd_xGa_2S_4$ crystals as new materials for mid-infrared parametric oscillators pumped by Nd :YAG lasers," Conference on Lasers and Electro-Optics CLEO'04, San Francisco (CA), USA, May 16-21, 2004, paper CThT44, CLEO/IQEC Technical Digest CD-ROM.

[14] Badikov, V. V., Don, A. K., Mitin, K. V., Seryogin, A. M., Sinaiskiy, V. V., and Schebetova, N. I., "Optical parametric oscillator on an $Hg_{1-x}Cd_xGa_2S_4$ crystal," Quantum Electron. **35**, 853-856 (2005) [transl. from Kvantovaya Elektron. **35**, 853-856 (2005)].

[15] Zondy, J.-J., Vedenyapin, V., Yelisseyev, A., Lobanov, S., Isaenko, L., and Petrov, V., "$LiInSe_2$ nanosecond optical parametric oscillator," Opt. Lett. **30**, 2460-2462 (2005).

[16] Petrov, V., Schunemann, P. G., Zawilski, K. T., and Pollak, T. M., "Non-critical singly resonant OPO operation near 6.2 μm based on a $CdSiP_2$ crystal pumped at 1064 nm," Opt. Lett. **34**, 2399-2401 (2009).

[17] Takaoka, E. and Kato, K., "Thermo-optic dispersion formula for $AgGaS_2$," Appl. Opt. **38**, 4577-4580, 1999.

[18] Beasley, J. D., "Thermal conductivities of some novel nonlinear optical materials," Appl. Opt. **33**, 1000-1003, 1994.

[19] Jayaraman, A., Narayanamurti, V., Kasper, H. M., Chin, M. A., and Maines, R. G., "Pressure dependence of the energy gap in some I-III-VI_2 compound semiconductors," Phys. Rev. B **14**, 3516-3519, 1976.

[20] Zondy, J.-J., Touahri, D., and Acef, O., "Absolute value of the d_{36} nonlinear coefficient of $AgGaS_2$: prospect for a low-threshold doubly resonant oscillator-based 3:1 frequency divider," J. Opt. Soc. Am. **14**, 2481-2497, 1997.

[21] Petrov, V., Badikov, V., and Panyutin, V., "Quaternary nonlinear optical crystals for the mid-infrared spectral range from 5 to 12 micron," In: *Mid-Infrared Coherent Sources and Applications*, ed. by M. Ebrahim-Zadeh and I. Sorokina, NATO Science for Peace and Security Series - B: Physics and Biophysics, Springer (2008), pp. 105-147.

[22] Zondy, J.-J., Petrov, V., Yelisseyev, A., Isaenko, L., and Lobanov, S., "Orthorhombic crystals of lithium thioindate and selenoindate for nonlinear optics in the mid-IR," In: *Mid-Infrared Coherent Sources and Applications*, ed. by M. Ebrahim-Zadeh and I. Sorokina, NATO Science for Peace and Security Series - B: Physics and Biophysics, Springer (2008), pp. 67-104.

[23] Schunemann, P. G., Zawilski, K. T., Pollak, T. M., Petrov, V., and Zelmon, D. E., "$CdSiP_2$: a new nonlinear optical crystal for 1 and 1.5-micron-pumped, mid-IR generation," Advanced Solid-State Photonics, Denver (CO), USA, Feb. 1 - 4, 2009, Conference Program and Technical Digest, Paper TuC6.

[24] Shileika, A., "Energy band structure and modulation spectra of $A^2B^4C^5_2$ semiconductors," Surf. Sci. **37**, 730-747, 1973.

[25] Nikogosyan, D. N., Nonlinear Optical Crystals: A Complete Survey, Springer (2005).

[26] Badikov, V. V., Kuzmin, N. V., Laptev, V. B., Malinovsky, A. L., Mitin, K. V., Nazarov, G. S., Ryabov, E. A., Seryogin, A. M., and Schebetova, N. I., "A study of the optical and thermal properties of nonlinear mercury thiogallate crystals," Quantum Electron. **34**, 451-456 (2004) [transl. from Kvantovaya Elektron. **34**, 451-456 (2004)].

[27] Zondy, J.-J., Yelisseyev, A., Lobanov, S., Isaenko, L., Petrov, V., Noack, F., and Rotermund, F., "$LiInSe_2$ nanosecond optical parametric oscillator," Conference on Lasers and Electro-Optics CLEO'05, Baltimore (MD), USA, May 22-27, 2005, paper CThQ5, CLEO/QELS Technical Digest CD-ROM.

[28] Wang, T.-J., Kang, Z.-H., Zhang, H.-Z., Feng, Z.-S., Jiang, Y., Gao, J.-Y., Andreev, Y. M., Lanskii, G. V., and Shaiduko, A. V., "Model and experimental inverstigation of frequency conversion in $AgGaGe_xS_{2(1+x)}$ (x=0,1) crystals," J. Phys. D: Appl. Phys. **40**, 1357-1362 (2007).

[29] Wang, T.-J., Zhang, H.-Z., Wu, F.-G., Feng, Z.-S., Zang, H.-Y., Kang, Z.-H., Jiang, Y., and Gao, J.-Y., "3-5 μm $AgGaS_2$ optical parametric oscillator with prism cavity," Laser Phys. **3**, 377-380 (2009).

[30] Brosnan, S. J. and Byer, R. L., "Optical parametric oscillator threshold and linewidth studies," IEEE J. Quantum. Electron. **QE-15**, 415-431 (1979).